Flame Length and Width Produced by Ejected Propane Gas Fuel from a Pipe

Osami Sugawa and *Kikuko Sakai*

Center for Fire Science and Technology Science University of Tokyo
2641 Yamasaki, Noda, Chiba 278 Japan

ABSTRACT

Flame tip height, width, and height to base of a lifted flame, formed by a ejected fuel gas through a pipe of $1/8B$, $1/4B$, $3/8B$, $1/2B$, $3/4B$, and $1B$, were observed as a function of dimensionless heat release rate. Fuel gas was supplied at the rate of $100\ell/min$, $200\ell/min$, and $400\ell/min$. Pipe heights from the ground level were set at $200mm$, $700mm$, and $1700mm$. Radiative heat fluxes were also measured at $0.1m, 0.27m, 0.71m, 1.1m, 1.27m, 1.71m, 1.9m, 2.9m$ from the pipe. Temperatures along the center line of the flame were measured. Dimensionless flame height. Ha/D, and dimensionless flame width, W_f/D were correlated well by 1/3 power of dimensionless heat release rate. Radiative heat fluxes to the dummy vessel were also estimated using the view factor and center-line temperature. Estimated radiative heat fluxes to the targets were compared with the measured ones and good agreement between them was obtained. This implies that the view factor on radiative heat flux to the target from a jet flame is useful to estimate the radiative heat flux to assess the fire safety.
KEYWORDS: jet flame, flame height, flame width, heat release rate, lifted flame, view factor.

1 INTRODUCTION

Fuel gas is supplied through piping networks in urban area but its suburbs propane gas, as a fuel gas for house use, is supplied by vessels of $20 \sim 30kg$. In order to get the higher cost performance and lower consumption of labor in the delivery service. in other words to get infrequent delivery service and lessen the numbers of vessels transported to houses, it is planned to set a big volume vessel of $1500kg$ in house yard (or in basement) and of which refuel will be made directly by connecting with a LPG bulk loll track. However, the setting of a big vessel in house yard may have high potential of fire risk in case of a neighbor fire occurred. Fire in neighbor may give radiative heat to the vessel and which may result high pressure and ejection of fuel jet. Pressure reduction is designed by the ejection of gas through a safety-pipe and bulb system so that jet flame will be generated on/above the nozzle of the pipe and which may feed extra radiative heat to the vessel and surroundings. It is demanded to assess the potential of radiative heat which may be fed from the jet flame to the vessel. In the first series of the experiment, the semi-full scale test had been carried out using a big vessel which was exposed to model fires (wood crib fires). Temperatures of vessel surface and its atmosphere were measured, and also function of a safety bulb for pressure reduction was verified [1]. In the second series of the test, fire safety assessment of the big vessel was carried out. And a part of the second test, basic information on a jet flame formed on a safety pipe is required, and we dealt with the measurements and observations on jet flame height, flame width, height to the base of lifted jet flame from a pipe, and radiative heat flux to the dummy vessel.

2 EXPERIMENTAL PROCEDURE

2.1 Piping and Experimental System

Figure 1 shows the outline of the layout of experiments. Fuel gas was let into the system through pressure reducers and valve system controlling the supply rate of $100\ell/min$,$200\ell/min$, and $400\ell/min$. The final flow rate of the piping system was monitored by a mass flow meter every $10sec$. Nozzle height were adjusted at $200mm$, $700mm$, and $1700mm$ high from the grand level. Fuel gas supply rates, pipe size with $mm\Phi$,nozzle height and dimensionless heat release rate designed are shown in Table 1.

2.2 Measurements and Observations

Temperatures in the ejected flame were measured along the center at $1m$, $2m$, $3m$, $4m$, $5m$, $6m$, and $7m$ high from the ground level. Radiation heat flux meters were set at $0.1m$, $0.27m$, $0.71m$, $1.1m$, $1.27m$, $1.71m$, $1.9m$, and $2.9m$ apart from the center of a pipe. Two sets of video system, focusing from North and East, were used for recordings of the flame images.

Table 1: Experimental Conditions

Experiment Number	Fuel Flow Rate (ℓ/min)	Bore Size (mm)	Nozzle Height (mm)	Q^* $(-)$
1	100	$1/8B$, $6.5mm$	700	3.99×10^4
2	$200 \rightarrow 180 \rightarrow 160$	$1/8B$, $6.5mm$	700	6.39×10^4
3	100	$3/8B$, $12.7mm$	700	7.48×10^3
4	200	$3/8B$, $12.7mm$	700	1.50×10^4
5	300	$3/8B$, $12.7mm$	700	2.25×10^4
6	400	$3/8B$, $12.7mm$	700	2.99×10^4
7	100	$1B$, $27.6mm$	700	1.07×10^3
8	200	$1B$, $27.6mm$	700	2.15×10^3
9	400	$1B$, $27.6mm$	700	4.30×10^3
10	400	$1/4B$, $9.2mm$	200	6.70×10^4
11	200	$1/4B$, $9.2mm$	200	3.35×10^4
12	100	$1/4B$, $9.2mm$	200	1.68×10^4
13	400	$3/8B$, $12.7mm$	200	2.99×10^4
14	200	$3/8B$, $12.7mm$	200	1.50×10^4
15	100	$1/2B$, $16.1mm$	200	4.14×10^3
16	200	$1/2B$, $16.1mm$	200	8.27×10^3
17	400	$1/2B$, $16.1mm$	200	1.65×10^4
18	400	$1B$, $27.6mm$	200	4.30×10^3
19	400	$3/4B$, $21.6mm$	200	7.93×10^3
20	200	$3/4B$, $21.6mm$	200	3.97×10^3
21	100	$1/8B$, $6.5mm$	1700	3.99×10^4
22	400	$1/4B$, $9.2mm$	1700	6.70×10^4
23	200	$1/4B$, $9.2mm$	1700	3.35×10^4
24	100	$1/4B$, $9.2mm$	1700	1.68×10^4
25	400	$3/8B$, $12.7mm$	1700	2.99×10^4
26	200	$3/8B$, $12.7mm$	1700	1.50×10^4
27	400	$1/2B$, $16.1mm$	1700	1.65×10^4
28	200	$1/2B$, $16.1mm$	1700	8.27×10^3
29	400	$3/4B$, $21.6mm$	1700	7.93×10^3
30	200	$3/4B$, $21.6mm$	1700	3.97×10^3
31	400	$1B$, $27.6mm$	1700	4.30×10^3

* In the test #2,gas supply rate was changed $200\ell/min$ to $160\ell/min$ with the changing rate of $20\ell/min$ to observe the blow-off of the flame.

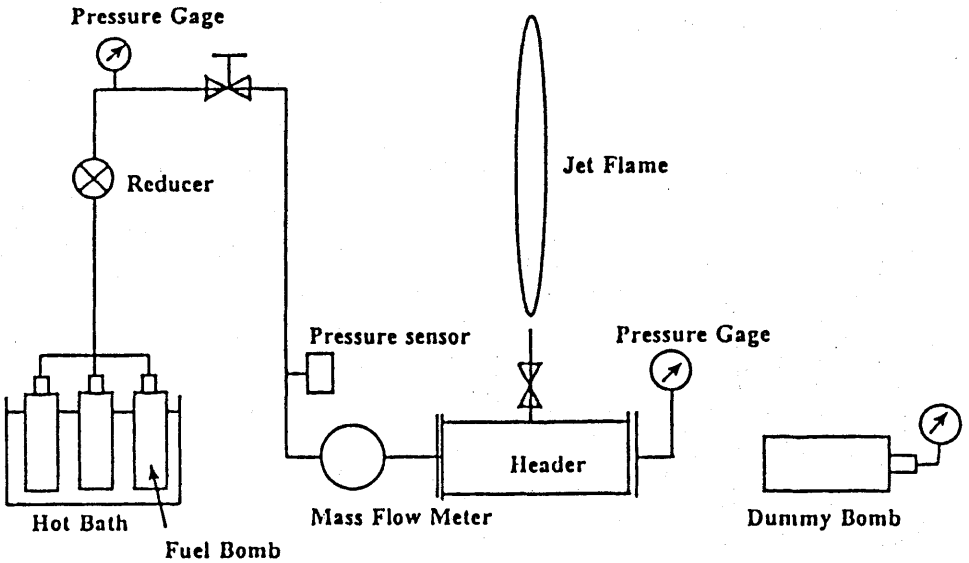

Figure 1 Outline of the experimental sets. Fuel gas vessels are set outside of the facility.Temperature along a jet flame and on the surface of the dummy vessel were measured by sheathed K-type thermocouples. Radiation meters were set on the same level of the dummy vessel.

3 RESULTS AND DISCUSSION

3.1 Flame Height and Width

Flame tip heights, Ha, were estimated from 90 successive images and are shown representatively in Figure 2 by a rigid line. In this case about $600kW$ $(400\ell/min)$ flame from $1/4B$ pipe was used, and the averaged flame tip height estimated was $3.04m$ with its maximum and minimum heights of $3.43m$ and $2.75m$, respectively. The difference between highest and lowest flame tip height was about $0.6m$ and of which standard deviation was about 10% of the full flame length. The flame width, W_f were estimated from the same images and are superimposed representatively in Figure 2 by a broken line. Standard deviation for W_f is about 20% and the fluctuation in both height and width of the flame is almost coincided with each other as shown in Figure 2. Average flame tip height, Ha, was normalized by pipe size, D, and are obtained in the dimensionless flame height of Ha/D. Figure 3 shows the logarithmic plots of dimensionless flame tip height, Ha/D, as a function of dimensionless heat release rate $Q^* = Q/\rho Cp\Delta T\sqrt{gD}D^2$ [4]. The figure indicates the relation of $Ha/D = 9.61 \cdot Q^{*1/3}$ for higher flame height, $Ha/D = 6.69 \cdot Q^{*1/3}$ for lower flame height, and $Ha/D = 8.14 \cdot Q^{*1/3}$ for average jet flame height for the range of Q^* of $10^3 \sim 6.7 \times 10^4$ based on the tests. The number of power, 1/3, for the relation is greater than that 0.23 which is reported by McCaffrey [2].

Flame widths, W_f, were also estimated and averaged based on 90 images and which was normalized by D as W_f/D. Figure 4 shows the relation of dimensionless flame width and Q^* in logarithmic scale. This figure shows W_f/D increased with the increase of $Q^{*1/3}$ and is expressed by $W_f/D = 1.92 \cdot Q^{*1/3}$. Figures 3 and 4 indicate that the characteristic flame length, both height and width, grows with $Q^{*1/3}$.

3.2 Height to the Base of Lifted Flame, h

Some of the tests showed the lifted flames. When we gave $200\ell/min$ and $180\ell/min$ to the $1/8B$ pipe, the lifted flame was observed once but it extinguished soon showing the lifting flame. In the case of ejection velocity exceeded $250m/sec$ at the bore resulted in the blow off of the flame. Except the test #2, we observed the stable flame with lifting. When lifted flame was observed, the height from the opening of pipe to the base of lifted flame, h, were estimated and averaged based on the 90 frames of successive images on the video system. Averaged one was normalized by pipe diameter, giving a dimensionless lifted height h/D, were plotted against Q^*. Figure 5 shows the h/D as a function of Q^* in $log - log$ scale, and which

implies that h/D increased with 3/5 power to Q^* in the region of $10^3 \sim 10^4$ and is expressed empirically by $h/D = 1.39 \times 10^{-2} \cdot Q^{*3/5}$.

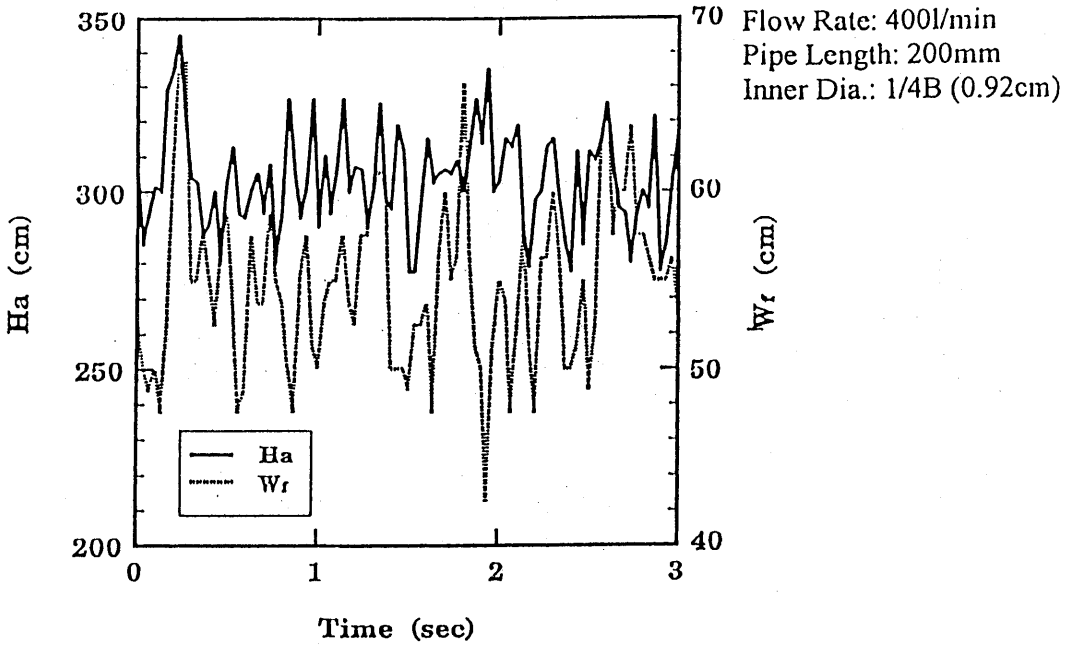

Figure 2 Typical time histories of flame tip height and its width. In this case, propane gas as a fuel was supplied at the rate of $400\ell/min$ from a $1/4B$ $(0.92cm\Phi))$ pipe of which length was $200mm$ from the ground.

3.3 Excess Temperatures, ΔT, along the Center Line of a Flame

In the lower region of a flame, $(Ha/D)/Q^{*2/5} \leq 2$, excess temperature, ΔT, showed almost constant of $850 - 950°C$ for the vertical direction. And ΔT decreased with $Ha^n (n = -3/2 \sim -5/3)$ for the region of $(Ha/D)/Q^{*2/5} > 2$. These gradients are quite similar to the ones obtained in the flame and plume in a diffusion flame as McCaffrey reported [3]. However, decreasing mode for intermittent, $(Z/Q^{2/5})^{-1}$, was not observed clearly in our tests as shown in Figure 6. Decreasing modes for vertical direction along the center line were characterized into two regions and are expressed by empirical equations as,
$\Delta T = \alpha \cdot ((Ha/D)/Q^{*2/5})^{*-3/2}$, where $\alpha = 1600°C$ for $(Ha/D)/Q^{*2/5} > 2$ and
$\Delta T = 850 \sim 950°C$ for lower flame region of "the base of flame" $\leq (Ha/D)/Q^{*2/5} \leq 2$.

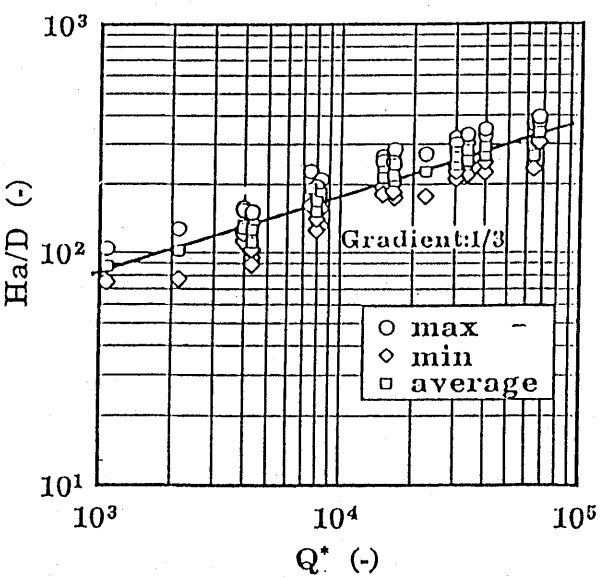

Figure 3 Logarithmic plots of dimensionless flame height, Ha/D, as a function of dimensionless heat release rate Q: with gradient of 1/3.

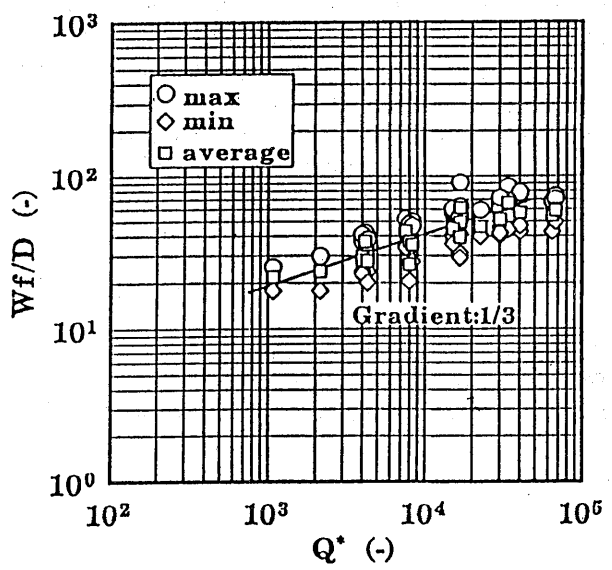

Figure 4 Dimensionless flame width, W_f/D, as a function of dimensionless heat release rate Q^*. W_f/D increased with 1/3 power of Q^*.

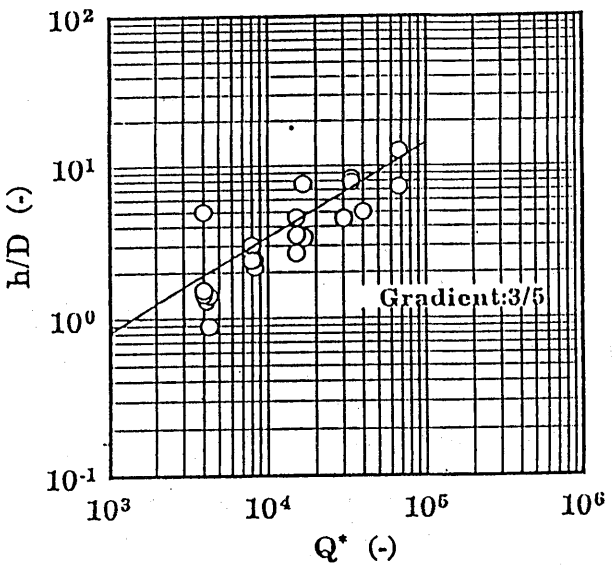

Figure 5 Dimensionless height to the base of lifted flame, h/D, are plotted against Q^* when no blow-off was observed.

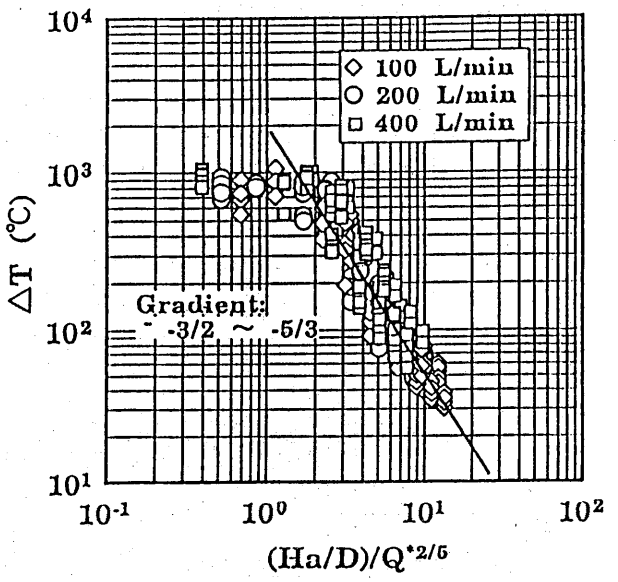

Figure 6 Excess temperatures along the center line of jet flame are plotted against normalized height by $Q^{*2/5}$. Vertical distribution of excess temperatures showed two regions with no decreasing and $-3/2 \sim -5/3$ power to the dimensionless height.

3.4 Radiation Heat Flux

Figure 7 shows the typical distribution profiles of radiation heat flux for horizontal direction with pipe heights of $200mm$, $700mm$, and $1700mm$. It is clearly observed that distribution of radiation heat flux showed flat in the near region from the pipe and then decayed in the far region.

In order to estimate the radiation heat flux to the vessel, we adopted following assumptions and two models for a jet flame to estimate the view factors between a flame and a target.

- Flame figure could be expressed by thin cylinder (including its bottom and of which view factor was presented in a text[5]) or by thin cone (or trapezoid) piled up to the average flame height, Ha, as shown in Figure 8-(a) and (b). Both models forms a conical flame in total shape.
- Maximum diameter of each cylindrical or trapezoidal flame appeared at the height of $0.9Ha$ and was estimated as a function of Q^* and D. Diameter at arbitrary height was estimated based on the angle of flame jet which was determined by D at Ha and the length to the base of the flame.
- Flame is translucent and its representative temperature at arbitrary heights can be estimated by

the empirical equation described along the center line.

Figure 7 also shows the representative distribution of radiative heat flux calculated based on the above flame models. This figure shows that the better coincidence was obtained between the estimated values and measured one if we adopt the cylindrical flame model than we adopt the trapezoidal model. The marginal part between flame and atmosphere is turbulent so that flat inclined surface of the trapezoidal flame model gave less radiation heat to the target.

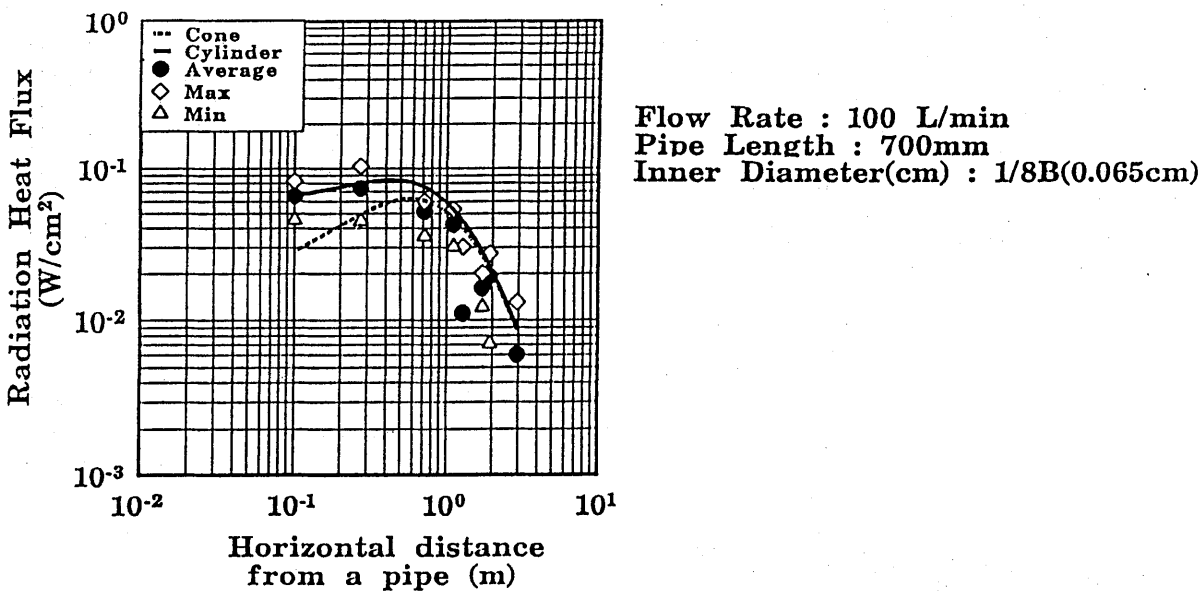

Figure 7 Horizontal distribution of radiation heat flux to the targets measured and calculated ones based on two models on jet flame figures illustrated in Figure 8-(a) and (b).

4 CONCLUSIONS

This work showed that the jet flame figures of height and width, and height to the base of lifted flame can be predicted by the power function of dimensionless heat release rate.

Excess temperature along the center line of the jet flame can be divided into two regions; lower flame region, and upper flame region. In the lower flame region ΔT showed almost constant of $850 \sim 950°C$, and upper flame regions,ΔT decreased with $-3/2 \sim -5/3$ power to the height. This decreasing rate is similar to the plume region of a diffusion flame from a pool fire. We observed no clear temperature decreasing mode of -1 power to height for the intermittent region.

It is important to note that the cylindrical flame piled up model, as shown in Figure 8-(a), indicates that the jet flame is translucent and has very turbulent marginal part between flame and atmosphere. The representative flame temperature is well approximated by the center line temperature. And the cylindrical flame model was better than trapezoidal model to estimate the radiation heat flux to the vessel from a jet flame.

5 ACKNOWLEDGEMENT

This work was supported financially by KHK (Kohatu-Gas Hoan Kyokai), and authors are grateful to Mr. T. Miura (KHK) and Mr. S. Ohsugi (Sci. Univ. of Tokyo) for their assistance in carrying out the experiments and observation on jet flame figures. One of authors (O.S.) wish to sincere acknowledge to Prof. Toshisuke Hirano (Tokyo Univ.) and Prof. Satoshi Ishizuka (Hiroshima Univ.) for their kind and valuable suggestions.

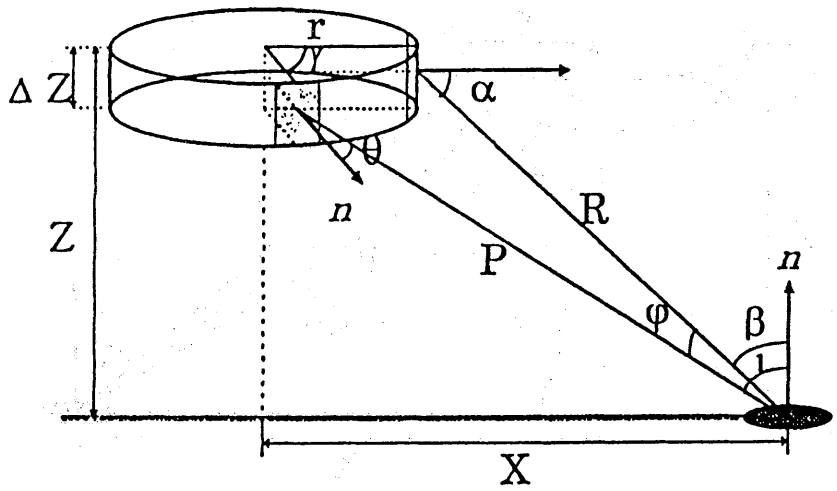

taking the lengths and angles in the above illustration,

$$\begin{aligned}
\mathbf{R} &= \sqrt{(\mathbf{X}-\mathbf{r})^2+\mathbf{Z}^2} \\
\mathbf{P} &= \sqrt{(\mathbf{X}-\mathbf{r}\cdot\cos\gamma)^2+(\mathbf{r}\cdot\sin\gamma)^2+\mathbf{Z}^2} \\
&= \sqrt{\mathbf{X^2}+\mathbf{r^2}+\mathbf{Z^2}-\mathbf{2X_r}\cdot\cos\gamma}
\end{aligned}$$

$$\cos\alpha=\frac{(\mathbf{X}-\mathbf{r})}{\mathbf{R}},\cos\beta=\frac{\mathbf{Z}}{\mathbf{R}},\cos\varphi=\frac{\sqrt{(\mathbf{D}-\mathbf{r}\cdot\cos\gamma)^2+\mathbf{Z}^2}}{\mathbf{P}}$$

the view factor F can be expressed as

$$\begin{aligned}
\mathbf{F} &= \int_{\mathbf{S}}\frac{\cos\theta\cdot\cos\iota}{\pi\cdot\mathbf{P}^2}\mathbf{dS} \\
&= \int_{\mathbf{S}}\frac{\cos\alpha\cdot\cos\gamma\cdot\cos^2\varphi\cdot\cos\beta}{\pi\cdot\mathbf{P}^2}\mathbf{dS} \\
&= \frac{\mathbf{2r}}{\pi}\int_0^{\mathbf{Z}}\int_0^{\frac{\pi}{2}}\frac{(\mathbf{X}-\mathbf{r})\cdot\cos\gamma\cdot[(\mathbf{X}-\mathbf{r})^2+\mathbf{Z}^2]\cdot\mathbf{Z}}{\mathbf{R^2}\cdot\mathbf{P^4}}\mathbf{d}\gamma\mathbf{dZ}
\end{aligned}$$

where

$$\begin{aligned}
\cos\theta &= \cos\gamma\cdot\cos\alpha\cdot\cos\varphi \\
\cos\iota &= \cos\varphi\cdot\cos\beta \\
\mathbf{dS} &= \mathbf{r}\cdot\mathbf{d}\gamma\cdot\mathbf{dZ}
\end{aligned}$$

Figure 8(a) Cylinder model for a jet flame to estimate the view factor.

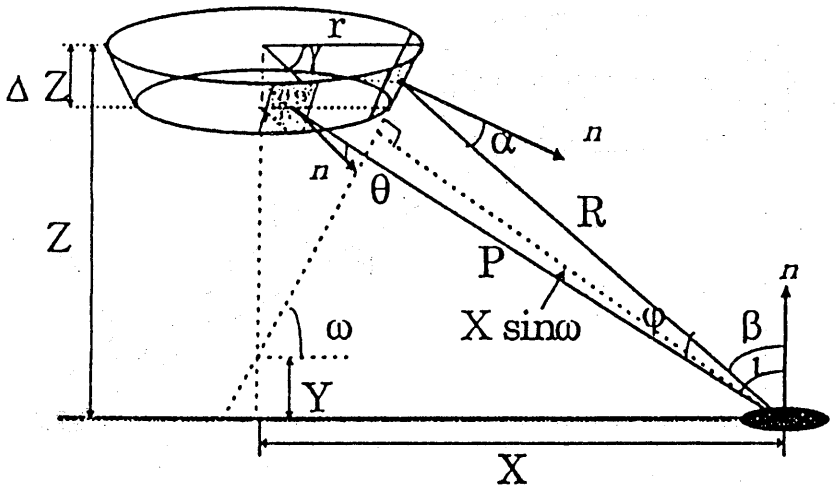

taking the lengths and angles in the above illustration,

$$\begin{aligned}
\mathbf{R} &= \sqrt{(\mathbf{X}-\mathbf{r})^2+\mathbf{Z}^2} \\
\mathbf{P} &= \sqrt{(\mathbf{X}-\mathbf{r}\cdot\cos\gamma)^2+(\mathbf{r}\cdot\sin\gamma)^2+\mathbf{Z}^2} \\
&= \sqrt{\mathbf{X^2}+\mathbf{r^2}+\mathbf{Z^2}-\mathbf{2X_r}\cdot\cos\gamma}
\end{aligned}$$

$$\cos\alpha = \frac{(\mathbf{X}+\frac{\mathbf{Y}}{\tan\omega})\cdot\sin\omega}{\mathbf{R}}, \cos\beta = \frac{\mathbf{Z}}{\mathbf{R}}, \cos\varphi = \frac{\sqrt{(\mathbf{D}-\mathbf{r}\cdot\cos\gamma)^2+\mathbf{Z}^2}}{\mathbf{P}}$$

the view factor F can be expressed as

$$\begin{aligned}
\mathbf{F} &= \int_{\mathbf{S}} \frac{\cos\theta\cdot\cos\iota}{\pi\cdot\mathbf{P}^2}\mathbf{dS} \\
&= \int_{\mathbf{S}} \frac{\cos\alpha\cdot\cos\gamma\cdot\cos^2\varphi\cdot\cos\beta}{\pi\cdot\mathbf{P}^2}\mathbf{dS} \\
&= \frac{\mathbf{2r}}{\pi}\int_0^{\mathbf{Z}}\int_0^{\frac{\pi}{2}} \frac{(\mathbf{X}+\frac{\mathbf{Y}}{\tan\omega})\cdot\cos\gamma\cdot[(\mathbf{X}-\mathbf{r})^2+\mathbf{Z}^2]\cdot\mathbf{Z}}{\mathbf{R^2}\cdot\mathbf{P^4}}\mathbf{d\gamma dZ}
\end{aligned}$$

where

$$\begin{aligned}
\cos\theta &= \cos\gamma\cdot\cos\alpha\cdot\cos\varphi \\
\cos\iota &= \cos\varphi\cdot\cos\beta \\
\mathbf{dS} &= \mathbf{r}\cdot\mathbf{d}\gamma\cdot\frac{\mathbf{dZ}}{\sin\omega}
\end{aligned}$$

Figure 8(b) Cone model for a jet flame to estimate the view factor.

6 REFERENCE

[1] Technical Report on 'Tank Temperatures exposed to Wood Crib Fires', Kohatsu-Gas Hoan Kyokai (KHK: High Pressure Gas Safety Association) Report (1994) (in Japanese)

[2] McCaffrey, B.J., 'Flame Height', Section 1/Chapter 18, The SFPE Handbook of Fire Protection Eng., First Edition, SFPE and NFPA (1988)

[3] McCaffrey, B.J. 'Purely buoyant diffusion flames: some experimental results'. NBSIR 79-1910 (1979)

[4] Zukoski, E. E., Kubota, T., and Cetegen, B. 'Entrainment in Fire Plumes', Fire Safety Journal, vol.3, pp. 107-121,(1980/81)

[5] for example, "Handbook of Chemical Engineering", Section 6.3, 5th Edition (1988) published by Maruzen (in Japanese)

7 NOMENCLATURE

D: bore size (m)

Ha: flame height from nozzle along the center line of a jet flame (m)

h: height to the base of lifted flame from bore (m)

AT: excess temperature from room temperature ('C or K)

W_f : width of jet flame (m)